Double negative metamaterials based on ferromagnetic microwires

Jorge Carbonell,* Héctor García-Miquel, and José Sánchez-Dehesa
Grupo Fenómenos Ondulatorios (GFO), Departamento de Ingeniería Electrónica, Universidad Politécnica de Valencia, Camino de Vera, s/n, 46022 Valencia, Spain

(Received 25 September 2009; revised manuscript received 19 November 2009; published 5 January 2010)

Ferromagnetic microwires are investigated as fundamental components to generate metamaterials with double negative parameters. Electric and magnetic responses are, respectively, based on the finite conductivity and ferromagnetic resonance of the wires that in turn depend on their chemical composition. Tuning properties of samples are investigated in terms of the composition of the alloy and the applied magnetic field. The samples are measured and simulated in a waveguide environment for a large microwave frequency range. Numerical modeling supports the experimental results and helps to understand the physics involved in the transmission phenomena. Radius and conductivity of the wires are pointed out as the most critical parameters to generate a double negative response in terms of permittivity and permeability.

DOI: 10.1103/PhysRevB.81.024401 PACS number(s): 41.20.Jb, 76.50.+g, 84.40.−x, 85.70.Ay

I. INTRODUCTION

During almost a decade, a huge amount of research has been devoted to the possibilities of controlling light propagation in microstructured media, typically made from subwavelength inclusions.[1] This broad area of research covering the whole spectrum of wave propagation from microwaves to optics, and even extended to acoustics,[2] has fueled the development and synthesis of the so-called metamaterials. Pioneering theories,[3] received renewed interest with the interpretation of refractive phenomena in artificial microstructures in terms of their electric[4] and magnetic activities.[5] On this basis, metamaterials have been basically driven by the development of microstructures relying on the artificial magnetism generated by split ring resonators (SRRs) or other types of current loops.[6–8] Nevertheless, this approach often requires the combination of two separate arrays being able to combine, in a given frequency range, a double (electric and magnetic) negative response. More recently, attention has been paid to the use of magnetic materials taking advantage of their magnetic activity to design double negative media.[9,10] In this case, solutions were also based on the combined use of ferrites and metallic wire arrays. In this context, it has been recently confirmed that an array of conducting ferromagnetic microwires can provide a double negative response, with experimental evidence of left-handed or backward wave propagation in the microstructure.[11] The ferromagnetic resonance (FMR) phenomenon in microwires, typically occurring at microwave frequencies, was previously studied in terms of material characterization, extraction of resonant permeability models or experimental investigation of resonating configurations.[12–15] These techniques have also been used in characterization of amorphous magnetic microwires.[16,17]

The originality of this work stems from the fact that we have measured a double negative propagation behavior in different prototypes made of single and multiple ferromagnetic microwires operating in different microwave bands from 8 to 18 GHz. The route using ferromagnetic inclusions permits one to increase the design capabilities with the use of the natural and tunable magnetic response of a ferromagnetic material. Tunability, a salient feature of this approach, is therefore addressed in a twofold manner. It is showed that very large tuning bandwidths are achievable by properly polarizing the samples with an external magnetic field, but also by varying the material composition of the wires forming the array. In addition to the experimental results, this work uses a numerical simulation model that, by precisely adapting the experimental parameters, recovers the measured transmission, reflection and absorption characteristics.

This paper is organized as follows. First, experimental results are presented including a description of the measurement setup and the ferromagnetic samples employed. Second, a numerical model including a complex description of the wire permeability is introduced to characterize the double negative physical phenomena involved in the transmission behaviors. Afterwards, both experimental and simulation data are analyzed and discussed in the light of the different physical phenomena involved, and the issues related to the use of these particular materials. Finally, a conclusions section summarizes the main results and findings of this work.

II. EXPERIMENTAL RESULTS

Glass coated amorphous microwires were prepared following the Taylor-Ulitovsky method[18] and have a general composition $(Co_{100-x}Fe_x)_{0.725}Si_{12.5}B_{15}$. Parameter x represents here the variable fraction of iron (and cobalt) in the alloy. In practice the authors have used samples with $x=0$ and $x=60$ to cover sufficiently different material compositions. The employed microwires have a ferromagnetic material core of radii ranging from 1.5 to 3.5 μm, due to the dispersion inherent to the fabrication method. Figure 1(a) shows a scanning electron microscope view of a sample microwire (glass coat partially removed). Different configurations with one and three wires have been analyzed in an experimental setup which is schematized in Fig. 1(b). In order to have a controlled measurement environment, and to avoid unwanted reflections, a waveguide mount has been preferred over a free space configuration. A hollow metallic waveguide is loaded with a number of wires in a row, centered with respect to the lateral walls and vertically oriented.

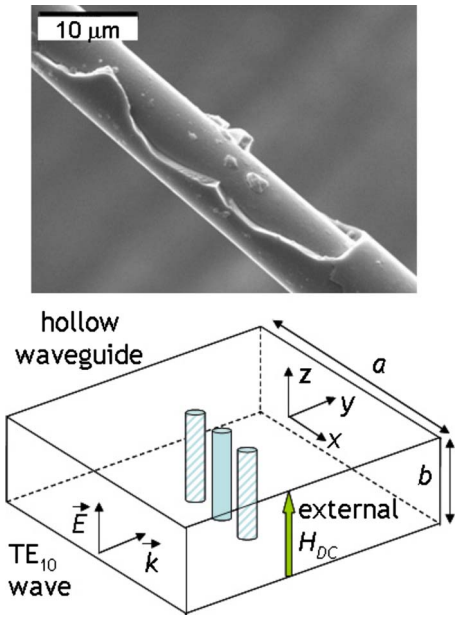

FIG. 1. (Color online) (a) Scanning electron microscopy view of a partially removed glass coat microwire, (b) Schematic view of the waveguide setup employed in the experiments for configurations including one or three wires.

Spatial separation of the wires is 4 mm. Since the waveguides are used in their respective TE_{10} dominant mode frequency range (*WR*-90 from 8 to 12 GHz and *WR*-62 from 12 to 18 GHz), the impinging wave has an electric field, e_{rf}, parallel to the wires and a magnetic field, h_{rf}, in the plane perpendicular to the wire axis. This setup is carefully analyzed in the following since h_{rf} has components in the transverse ($\vec{x}$) and longitudinal directions ($\vec{y}$), both perpendicular to the wire axis. In any case, the cylindrical symmetry of the wires is an advantage over the use of a SRR, which is in essence anisotropic. The wire or wires are stuck on a slab of Rohacell foam, which in turn can also be stacked to form prototypes with multiple layers. This foam is selected since it is neutral in practice to the EM radiation ($\varepsilon_r = \mu_r = 1$) and acts as a support for the wires.

The experimental setup is working in two frequency bands so that different size waveguides and transitions are used. A full two port through-reflect-line calibration is performed in both cases. Transmission and reflection coefficients are measured in terms of *S* parameters with a Rohde&Schwarz ZVA-24 network analyzer. The prototype samples filling the waveguides are polarized with an external electromagnet delivering a static magnetic field $\mathbf{H_{dc}}$. This field is polarized parallel to the axis of the wires [see Fig. 1(b)]. The variation of the field intensity is measured with a probe located as close as possible to the position of the sample.

Figures 2 and 3 show, respectively, the measured parameters for a single wire structure with $x=0$ and $x=60$, varying the applied external static field $\mathbf{H_{dc}}$. From the measured transmission (S_{21}) and reflection (S_{11}), the measured coefficient of power absorption P_{abs} is calculated as:

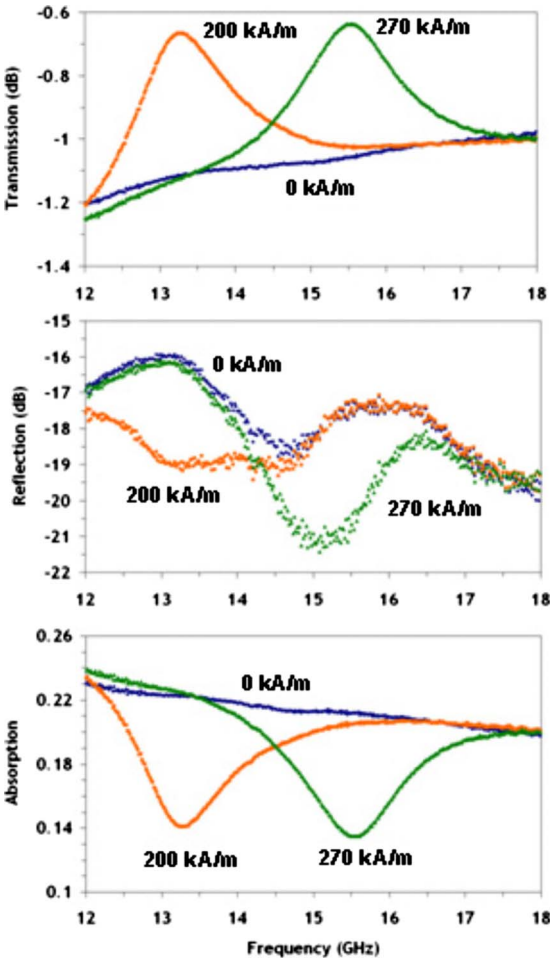

FIG. 2. (Color online) Transmission, reflection and absorption coefficients measured for a single wire sample with $x=0$.

$$P_{abs} = 1 - |S_{11}|^2 - |S_{21}|^2. \quad (1)$$

Comparing both cases ($x=0$ and $x=60$), results show coherent evolutions. Transmission without polarization ($\mathbf{H_{dc}} = 0$ kA/m) shows an increase with frequency, while reflection follows the opposite trend. This behavior is attributed to the conducting properties of the wires, even if the alloy has a moderate conductivity. The transmission increase with frequency is the one of a metallic wire short circuiting the waveguide. Since it is of very small radius, the mean transmission level remains high (small reflecting obstacle). Once a magnetic field $\mathbf{H_{dc}}$ is applied, the transmission curves show an increased transmission window related to the double negative condition obtained in the wire. It is important to underline that the double negative behavior is produced for a single wire structure. Therefore, it is not necessary to have an array to observe the basic behavior. However, configuring a sample in the form of an array may permit designing a device with engineered characteristics as it is usually achieved with other metamaterial microstructures. It is also important to note that absorption is reduced in the transmitted band with respect to the nonpolarized situation. Comparing both samples, it is seen that the value of $\mathbf{H_{dc}}$ necessary to obtain the transmission band in the 12–18 GHz range is double in

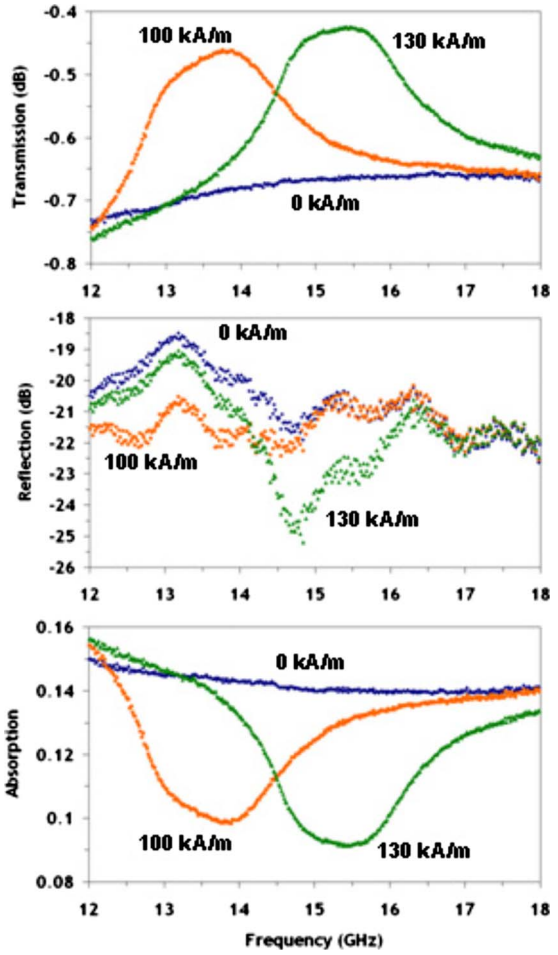

FIG. 3. (Color online) Transmission, reflection and absorption coefficients measured for a single wire sample with $x=60$.

the $x=0$ case, with respect to the $x=60$ case. This is basically due to magnetic anisotropy and the different saturation magnetization M_s of the samples.[17] This parameter is dependent on the chemical composition of the wire core, $M_{s(x=0)}=0.55$ T and $M_{s(x=60)}=0.97$ T. This factor of approximately 2 between both values can be recovered from the necessary magnetic field values to be applied to both wires to obtain a similar resonance frequency. Therefore, composition of the wires can be an extra tuning parameter in addition to the external magnetic field.

III. NUMERICAL MODELING

For the interpretation of the experimental data, the finite element simulation code Comsol Multiphysics has been employed. With respect to the geometry, the authors have used a two-dimensional (2D) simulation scheme assuming invariance in the z direction; see Fig. 1(b). The metallic walls (top and bottom) of the waveguide are considered symmetry boundaries and therefore the real setup can be reduced to a 2D problem. The wire can be considered of infinite length, provided that there is an electrical contact with the top and bottom walls in the real environment. An issue also to take into account is the very large aspect ratio between the transverse dimension of the waveguide ($a=15.8$ mm for the *WR*-62 waveguide and $a=22.86$ mm for the *WR*-90) and the wire diameter (which is taken $2r=4$ μm). The meshing inside the wire and of its surrounding area has to be very dense in order to capture the intense field variations produced especially at the resonance frequency.

The modeling of the material properties of the microwires has been realized simultaneously considering both characteristics in terms of electric and magnetic responses. As stated previously, the electrical response of the wires is related to the finite conductivity of the alloy composition. A fixed value of $\sigma=6.7$ 10^5 S/m is assigned to the wire region (for the $x=0$ sample). This approach is equivalent to the one employed for example in,[19] where a permittivity function was used instead. At microwave frequencies, where the ferromagnetic resonance effects occur, the authors assume that conductivity is a good and stable magnitude to model the electric response of the wires. The conductivity of the amorphous ferromagnetic alloy is smaller than the one of a crystalline alloy. Its moderate value will increase the skin depth and hence the penetration of electromagnetic fields inside the wires. It is known (see for example[4]) that for bulk conductors a negative real permittivity can be defined according to a Drude-like model. Also, the effective permittivity associated to a conducting wires microstructure has an equivalent model (also based on a Drude-like response) taking into account also the geometric parameters of the structure. Finally, this permittivity is applicable in our case since e_{rf} of the excitation wave is parallel to the microwires in our setup, and they behave as infinite length conductors (they short circuit the waveguide).

The magnetic response is much more complex and is essentially driven by the FMR phenomenon associated to the wires. As qualitatively proposed in,[11] the magnetic response of the microwires can be modeled with a Lorentz-type behavior defined by the characteristic parameters of the wires (including in particular losses) and the external applied field $\mathbf{H_{dc}}$. Since the excitation wave is the TE_{10} mode of the waveguide, the high-frequency magnetic field, h_{rf}, will have both components in the $\vec{x}$ and $\vec{y}$ directions; see Fig. 1(b). The relative magnetic permeability μ, and the dynamic susceptibility χ, of the bulk material employed in the simulation can be described with the following tensor model:[20]

$$\mu = 1 + \chi = \begin{pmatrix} \mu_{xx} & \mu_{xy} \\ \mu_{yx} & \mu_{yy} \end{pmatrix} = \begin{pmatrix} 1 + (X_p - iX_s) & i(K_p - iK_s) \\ -i(K_p - iK_s) & 1 + (X_p - iX_s) \end{pmatrix},$$

where the susceptibility elements are found to be

$$X_p = \frac{\omega_0\omega_m(\omega_0^2 - \omega^2) + \omega_0\omega_m\omega^2\alpha^2}{[\omega_0^2 - \omega^2(1+\alpha^2)]^2 + 4\omega_0^2\omega^2\alpha^2},$$

$$X_s = \frac{\omega\omega_m\alpha(\omega_0^2 + \omega^2(1+\alpha^2))}{[\omega_0^2 - \omega^2(1+\alpha^2)]^2 + 4\omega_0^2\omega^2\alpha^2},$$

$$K_p = \frac{\omega\omega_m(\omega_0^2 - \omega^2(1+\alpha^2))}{[\omega_0^2 - \omega^2(1+\alpha^2)]^2 + 4\omega_0^2\omega^2\alpha^2},$$

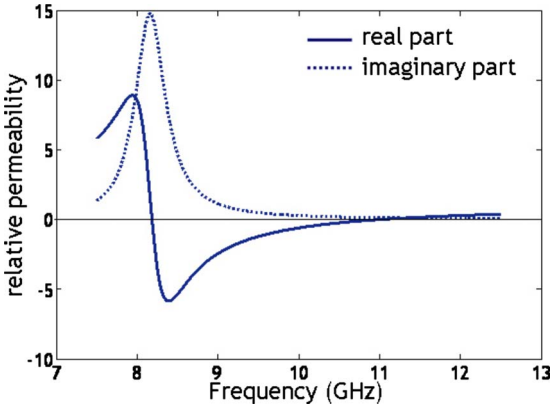

FIG. 4. (Color online) Permeability model for the $x=0$ microwire samples with real μ' and imaginary μ'' parts (external applied magnetic field is $\mathbf{H_{dc}}=100$ kA/m), demagnetization factors are taken as $N_x=1$ and $N_y=0$.

$$K_s = \frac{2\omega^2\omega_0\omega_m\alpha}{[\omega_0^2 - \omega^2(1+\alpha^2)]^2 + 4\omega_0^2\omega^2\alpha^2},$$

and $\omega_m=\mu_0\gamma M_s$ is the resonance frequency at the saturation limit, $\gamma=1.93\ \ 10^{11}\ \ \mathrm{T}^{-1}$ $(g=2.2)$,[17] is the gyromagnetic ratio, and $\omega_0=\mu_0\gamma H_0$ is the Larmor resonance frequency. A dimensionless damping factor, taking into account magnetic losses, is set to $\alpha=0.02$, by fitting the experimental data. It is essential to note that the above model does not consider the actual geometry, since it defines the bulk susceptibility applied to the wire region of the simulation domain. Nevertheless, the simulation results take into account the geometry dependent characteristics of the resonance phenomena by meshing the inside of the wire and calculating the full-wave patterns. In particular, demagnetization factors ($N_x=1$ and $N_y=0$), related to the cylindrical geometry of our samples can be used to theoretically predict the FMR frequency, given by the expression

$$\omega_{FMR} = \mu_0\gamma\sqrt{(H_0 + N_xM_S)(H_0 + N_yM_S)}.$$

Given the cylindrical geometry, the wire radius and the operation frequencies, the previous model can be adapted to plot the effective permeability of the microwire. A plot showing the effective permeability values for the principal directions, with their real and imaginary parts, is given in Fig. 4. In this model, actually introduced in,[11] the salient feature is the range of permeability values having a negative real part. This happens between the FMR and antiresonance (FMAR) frequencies, where permeability has null values. According to this model, FMR frequency of the $x=0$ sample occurs at 8.2 GHz for $H_0=100$ kA/m. The antiresonance frequency is approximately at 11 GHz. A wide frequency range falls under this condition, necessary to create a double negative medium.

IV. ANALYSIS AND DISCUSSION

A comparison between measured and simulated results is given in Fig. 5. Data for a three-wire configuration [see Fig. 1(b)] are displayed in terms of the transmission, reflection and absorption coefficients at different polarization magnetic fields in a *WR*-90 waveguide (8–12 GHz). Sample microwires have in this case a chemical composition of $Co_{72.5}Si_{12.5}B_{15}$, with $x=0$. Figure 5 shows that a relatively good agreement is found between theoretical and experimental results, demonstrating that the theoretical model captures the physics behind this experiment. It is shown that the model approximately predicts the frequency variations related to the application of an external magnetic field. They are basically related to H_0, M_s, and γ. Also, maximum values of the transmission and reflection coefficients can be recovered especially if the parameters related to the losses are adjusted.

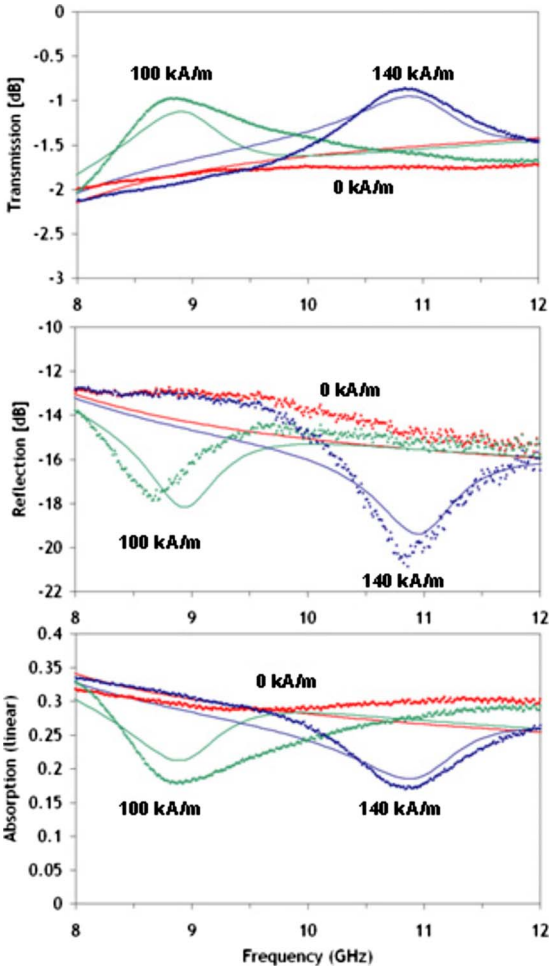

FIG. 5. (Color online) Compared simulation (lines) and experimental (symbols) results for a 3 wires structure in terms of transmission, reflection and absorption coefficients.

Finally, the observed decrease of the absorption coefficient corresponding to the transmission window is also predicted by the theoretical model. The decrease in absorption is associated to the fact that the skin depth is comparable to the wire radius (thick wires act as reflectors). Simulations with thicker wires show significantly different behaviors. The transmission window is produced in the region where double negative values of permittivity and permeability coexist. The wire conductivity locally generates a negative permittivity value, as it happens in general for metals at microwave fre-

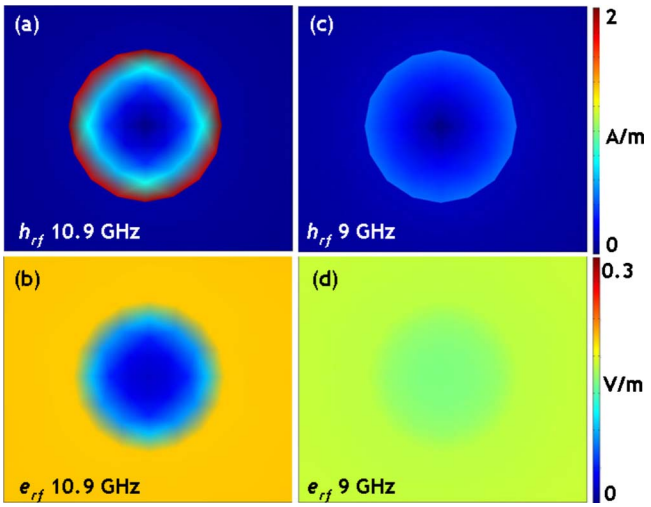

FIG. 6. (Color online) Magnitude of magnetic (a)–(c) and electric (b)–(d) field plots in the area around the central wire of the array (three wires with $x=0$) at 10.9 and 9 GHz, for an applied magnetic field of $\mathbf{H_{dc}}=140$ kA/m and a normalized TE_{10} incident wave of 1 mW of power.

quencies. This is a broadband response. However, permeability is negative only in a reduced part of the spectrum, between FMR and FMAR, which corresponds to the 8.2–11 GHz band.

Figure 6 shows the e_{rf} and h_{rf} amplitude patterns in the vicinity of the central wire in the three-wire array, when an external magnetic field $\mathbf{H_{dc}}=140$ kA/m is applied. The fields are plotted at two frequencies: 10.9 and 9 GHz. The first frequency corresponds to the maximum transmission, as from Fig. 5; and second frequency is almost out of the increased transmission range. The influence of the small wire radius is clearly visible since the EM field fully penetrates inside the wire. The resonance feature, which is clearly visible in the magnetic field, is only slightly observable in the electric field. Skin depth δ is comparable to the wire radius ($r=2$ μm), assuming that $\delta=\delta_0/\sqrt{\mu_r}$ and $\delta_0(10\ \text{GHz})=6$ μm. Uniform e_{rf} field values are obtained inside the wire at both frequencies. At 10.9 GHz, the wire section exhibits an important magnetic field variation related to the FMR phenomenon, with extreme values on the wire border. To obtain the enhanced transmission it is very important that the radius of the wires is small (comparable to the skin depth) in order to produce a good interaction between the EM wave and the ferromagnetic core. If this radius is large, the inner part of the wires will not interact with the EM wave and will behave as a simple conductor that produces a reflection of the EM wave.

Finally, it is worth mentioning that electric (associated to the moderate conductivity σ) and magnetic (associated to the damping factor α) losses rapidly degrade the transmission level with the number of wires. Devices based on a large number of wires absorb a large part of the EM energy of the excitation wave. For practical purposes, this is the main drawback of this type of technology. Other authors have very recently proposed reduced loss solutions but these are based on the use of the combination of dielectric and ferromagnetic materials.[21]

V. CONCLUSION

In this paper, an experimental and numerical analysis of different configurations of ferromagnetic microwires in a waveguide environment has been presented. Transmission, reflection and absorption coefficients have been measured for different compositions of the microwires and with different applied magnetic fields, covering a wide frequency range. The tunability of the proposed structures is of great relevance in the metamaterial context, owing to the possibility of extending the operation bandwidths. Experimental results have been explained in terms of a theoretical model that captures the underlying physics by properly characterizing a double negative response, in terms of effective permittivity and permeability. Small radius and moderate conductivity of the microwires are key elements to obtain the desired effect. It is therefore concluded that a ferromagnetic wire can be considered as the unitary constituent of a double negative medium.

ACKNOWLEDGMENTS

The authors acknowledge the financial support of Ministerio de Ciencia e Innovación (Grants No. TEC 2007-67239 and No. Consolider CSD2008-00066) and Generalitat Valenciana (Grants No. GV/2007/215 and No. GVPRE/2008/007).

*Author to whom correspondence should be addressed; jorcarol@upvnet.upv.es

[1] *Metamaterials. Physics and Engineering Explorations*, N. Engheta and R. W. Ziolkowski (Wiley Inter-Science, IEEE Press, Piscataway, NJ, 2006).
[2] D. Torrent and J. Sanchez-Dehesa, Phys. Rev. Lett. **103**, 064301 (2009).
[3] V. G. Veselago, Sov. Phys. Usp. **10**, 509 (1968).
[4] J. B. Pendry, A. J. Holden, W. J. Stewart, and I. Youngs, Phys. Rev. Lett. **76**, 4773 (1996).
[5] J. B. Pendry, A. J. Holden, D. J. Ribbins, and W. J. Stewart, IEEE Trans. Microwave Theory Tech. **47**, 2075 (1999).
[6] J. D. Baena, L. Jelinek, and R. Marqués, Phys. Rev. B **76**, 245115 (2007).
[7] H. Chen, L. Ran, J. Huangfu, X. Zhang, K. Chen, T. M. Grzegorczyk, and J. A. Kong, Appl. Phys. Lett. **86**, 151909 (2005).
[8] F. Zhang, S. Potet, J. Carbonell, E. Lheurette, O. Vanbesien, X. Zhao, and D. Lippens, IEEE Trans. Microwave Theory Tech. **56**, 2566 (2008).
[9] H. Zhao, J. Zhou, Q. Zhao, B. Li, and L. Kang, Appl. Phys. Lett. **91**, 131107 (2007).
[10] H. Zhao, J. Zhou, L. Kang, and Q. Zhao, Opt. Express **17**, 13373 (2009).
[11] H. Garcia-Miquel, J. Carbonell, V. E. Boria, and J. Sanchez-Dehesa, Appl. Phys. Lett. **94**, 054103 (2009).
[12] Charles Kittel, Phys. Rev. **73**, 155 (1948).

[13] C. E. Patton, Z. Frait, and C. H. Wilts, J. Appl. Phys. **46**, 5002 (1975).
[14] S. E. Lofland, S. M. Bhagat, H. L. Ju, G. C. Xiong, T. Venkatesan, R. L. Greene, and S. Tyagi, J. Appl. Phys. **79**, 5166 (1996).
[15] N. Bloembergen, Phys. Rev. **78**, 572 (1950).
[16] H. Garcia-Miquel, M. J. Esbrí, J. M. Andrés, J. M. Garcia, J. M. Garcia-Beneytez, and M. Vázquez, IEEE Trans. Magn. **37**, 561 (2001).
[17] S. E. Lofland, H. García-Miquel, M. Vázquez, and S. M. Bhagat, J. Appl. Phys. **92**, 2058 (2002).
[18] H. García-Miquel and M. Vazquez, Physica B **299**, 225 (2001).
[19] J. Chen, D. Tang, B. Zhang, Y. Yang, M. Lu, H. Lu, F. Lu, and W. Xu, J. Appl. Phys. **102**, 023106 (2007).
[20] R. E. Collin, *Foundations for Microwave Engineering*, 2nd ed. (McGraw-Hill, New York, 1992).
[21] F. Xu, Y. Bai, L. Qiao, H. Zhao, and J. Zhou, Appl. Phys. Lett. **95**, 114104 (2009).